



ELSEVIER

Deep-Sea Research II 52 (2005) 615–625

DEEP-SEA RESEARCH  
PART II

[www.elsevier.com/locate/dsr2](http://www.elsevier.com/locate/dsr2)

# On the Deep Western Boundary Current south of Cape Cod

Terrence M. Joyce\*, Jane Dunworth-Baker, Robert S. Pickart,  
Daniel Torres, Stephanie Waterman

*Woods Hole Oceanographic Institution, Mail Stop 21, 360 Woods Hole Road, Woods Hole, MA 02543, USA*

Received 13 April 2004; accepted 2 December 2004

## Abstract

Using CTD/oxygen data from eight cruises in the decade from 1994–2003, we have constructed a mean ‘section’ of properties across the Deep Western Boundary Current (DWBC) south of Cape Cod near 70°W. Since all sections included direct velocity measurements, our composite section enables us to portray the flow field as well as the mean water mass structure. Inshore of the Gulf Stream between the 2500 and 4000 m isobaths, the flow is to the southwest along the bathymetry and is remarkably barotropic. The equatorward flowing Labrador Sea Water is shown to have high dissolved oxygen, low salinity, and low potential vorticity, while the underlying Overflow Water is high in oxygen. Transport estimates for the cold limb of the thermohaline circulation give a range of  $-14$  to  $-19$  Sv for the N. Atlantic Deep Water found on the section. The greatest uncertainty is due to the presence of a Warm-Core Ring on one of the sections, which apparently completely reversed the flow in the DWBC. Offshore of the DWBC, some of the deep source waters are returned to the north in the deep Gulf Stream. The section is compared to two other, widely separated locations (Abaco and 55°W) that have markedly different DWBC characteristics.

© 2005 Elsevier Ltd. All rights reserved.

## 1. Introduction

The flow and properties of the Deep Western Boundary Current (DWBC) change significantly during its transit through the N. Atlantic Ocean. At 55°W, Pickart and Smethie (1998) show the core of maximum equatorward flow of Labrador Sea Water (LSW), and Iceland and Denmark Strait Overflow Water largely coincides with the

tracer cores of salinity, potential vorticity (PV), and oxygen. We define PV to be  $(-f/\rho_\theta)(\partial\rho_\theta/\partial z)$ . Equatorward transports of these deep density classes were estimated (from four cruises) to be  $-18.9 \pm 6.3$  Sv and are mostly found over sloping bathymetry between 2000 and 4000 m depth. In contrast, offshore of Abaco at 26.5°N, Leaman and Harris (1990) found the deep equatorward flow over relatively flat topography with a much greater transport ( $-34.8 \pm 14.5$  Sv). In both cases, the error bars are based on the sample standard deviation, not the error of the ‘mean’. In the Abaco section, the issue of deep recirculation was

\*Corresponding author. Tel.: +001 508 289 2530;  
fax: +001 508 457 2181.

E-mail address: [tjoyce@whoi.edu](mailto:tjoyce@whoi.edu) (T.M. Joyce).

raised to explain the discrepancy between the measured transport and that estimated from tracer measurements (Fine and Molinari, 1988). Deep recirculation, as pointed out by Schmitz and McCartney (1993), could dominate the actual near-boundary transport, swamping the smaller net throughflow of the deep water. The Pickart and Smethie estimates are not immune to effects of deep recirculation, although Hogg et al. (1986) place the northern recirculation gyre of the Gulf Stream in somewhat deeper water than the DWBC flow as noted by Pickart and Smethie (1998).

We study a third site between the above two, at 70°W, before the DWBC crosses under the Gulf Stream. This site has been relatively well measured with hydrographic cruises having direct velocity measurements, which we will see are essential to defining the deep transport. The cruises (Table 1) span a 10-year period from 1994–2003, and were taken mostly for other purposes than to estimate the transport and structure of the DWBC. However, the repeated measurement of tracers such as oxygen (and salinity), and direct velocity measurements with a Lowered Acoustic Doppler Current Profiler (LADCP) have provided an opportunity to construct a ‘mean’ section at this location as well. As this site is now instrumented for a four-year period of deep transport measurements from moorings ([http://www.whoi.edu/institutes/occi/currenttopics/ct\\_oms\\_stationw.html](http://www.whoi.edu/institutes/occi/currenttopics/ct_oms_stationw.html)), this summary represents what is known about the structure

and transport of the DWBC prior to the array deployment.

## 2. Data discussion and mean property sections

Station data from eight cruises (Table 1) and from a one-year deployment of a moored profiler mooring (Doherty et al., 1999) include CTD/LADCP stations taken at a number of sites over a period of years. The station velocity data have been obtained with a LADCP, and have been processed using standard methods (Fischer and Visbeck, 1993). Hydrographic data were collected with a Conductivity, Temperature, ‘Depth’, Oxygen (CTDO<sub>2</sub>) instrument, with salinity and oxygen calibrated to water samples collected on a Rosette. We show the position of these stations in Fig. 1, which define a “line” roughly normal to the bathymetry, starting at the shelf break and extending seaward into the Sargasso Sea. A least square fit to a straight line determines the local distance and depth for each station relative to an origin (shown in Fig. 1). Most stations were in shallow (<3000 m) water; our ensemble for deeper depths is rather small, reducing to two cruises from 4000 m out to 4500 m water depth, and one cruise beyond that. Only two cruises sampled far enough offshore to encounter the Gulf Stream, and only one (the last) sampled across it into the Sargasso Sea. Thus, our ensemble will represent varying degrees of freedom as we construct mean property sections. Velocity data are decomposed into parallel and normal components to our section, and a filter with Gaussian half-widths of 25 km (in the horizontal) and 50 m (in the vertical) is used to define weights for gridding onto a regular distance depth grid. Etop05 minute resolution bathymetry was linearly interpolated to determine local water depths and to define a depth/distance ‘mask’ for use with section plots and when estimating volume transports. The moored profiler, located at the 3000 m isobath, was given an equivalent weight of 10 stations, as it represented a one-year mean for the location.

From the mean of the measured temperature and salinity, potential temperature, neutral density, and potential vorticity (ignoring relative

Table 1  
Summary of cruises providing data

Line	W Cruise Table	Comment
Cruise	Date	
en257	Nov-94	10 stas., BOUNCE
oc269	Jun-95	4 stas., 3 w/LADCP, BOUNCE
en283	May-96	7 stas., PRIMER
en286	Aug-96	8 stas., PRIMER
en295	Feb-97	5 stas., PRIMER
en311	Dec-97	6 stas., WCR present, PRIMER
oc371	Oct-01	4 stas., deploy “W” mooring
station W	Sep-02	end of 1 year-long average at “W”
kn173_2	Oct-03	17 stas., Repeat Hydro.

When part of a larger program, these project names are given in the third column.

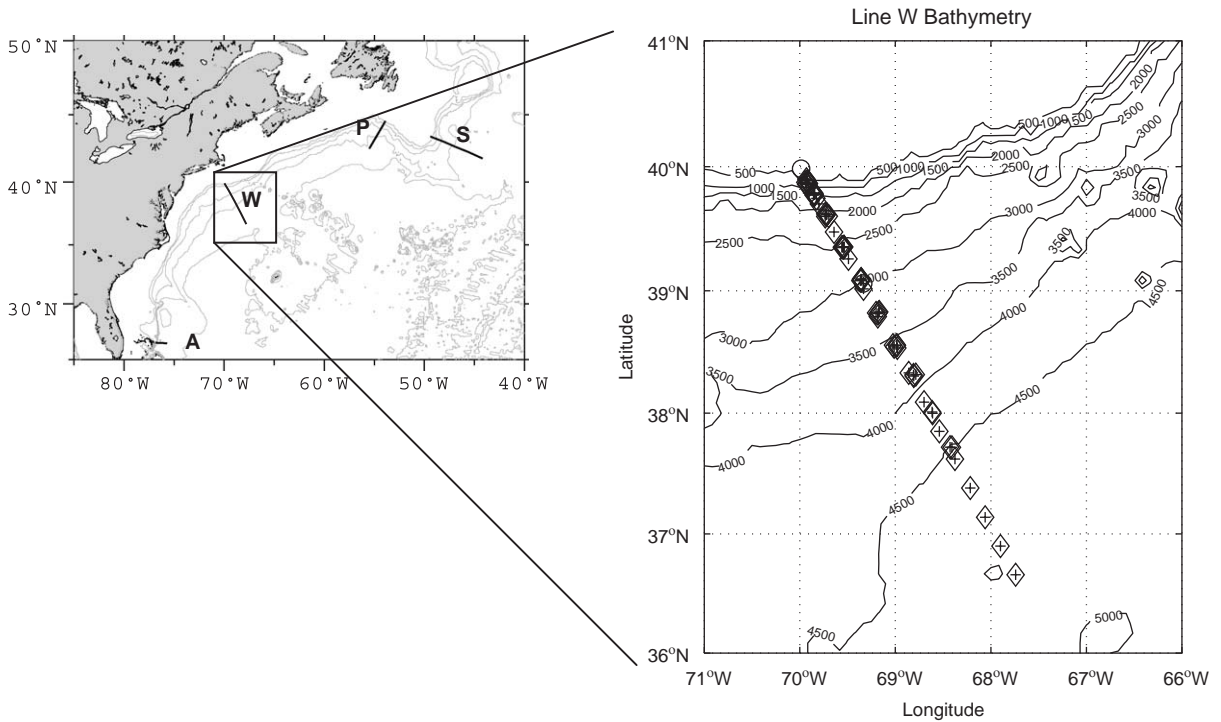


Fig. 1. Various regions where DWBC observations discussed have been made (left panel, bathymetric contour interval 1000 m). Letters refer to our work (W), Abaco (A), Pickart & Smethie (P) and Schott et al. (S). Our region of focus (right panel, bathymetric contour interval 500 m) is south of Cape Cod, between the upstream locations near the Grand Banks of Newfoundland, and the downstream site to the east of Florida. The circle symbol, at the inshore edge of the collection of stations used in defining a mean cross section, is taken to be the ‘origin’ of our coordinate system. It is located at a depth of 210 m at the shelf break.

vorticity) were then estimated. Density levels appropriate to define the LSW and Overflow/Lower Deep Water (LDW) were then taken to define boundaries for vertical integration of cross-stream velocity (transport), which will be presented in the next section.

The ensemble-average hydrographic structure as a function of distance offshore of the shelf break is given in Figs. 2 and 3. In the upper 500 m, the potential temperature and salinity clearly show their most rapid changes upon entering the Gulf Stream (offshore distance of ca. 250 km). Within the Gulf Stream, large positive velocities are found with mean values above 80 cm/s. One can see from the sections that although Sargasso Sea Water is encountered at the far right of the section (note the salinity maximum and the thickening of the temperature contours associated with Eighteen Degree Water), it is still within the poleward

surface jet, and density surfaces continue to deepen in the offshore direction at the offshore extremity of the section.

The deeper levels of North Atlantic Deep Water (NADW) are our main interest here, as they are involved with the transport of low-salinity, high-oxygen waters from the Labrador Sea, and high-oxygen overflow waters. At inshore depths along the continental slope, one can see evidence for more pristine versions of these water masses, with evidence for the water-mass signal deepening offshore along density surfaces and slowly losing its signature as one crosses the deep Gulf Stream. The low PV signal associated with the convectively formed LSW clearly stands out as a useful water-mass signature.

As discussed by Pickart and Smethie (1993), the effect of Topographic Rossby Waves (TRWs), which have wavelengths of 100 km and amplitudes

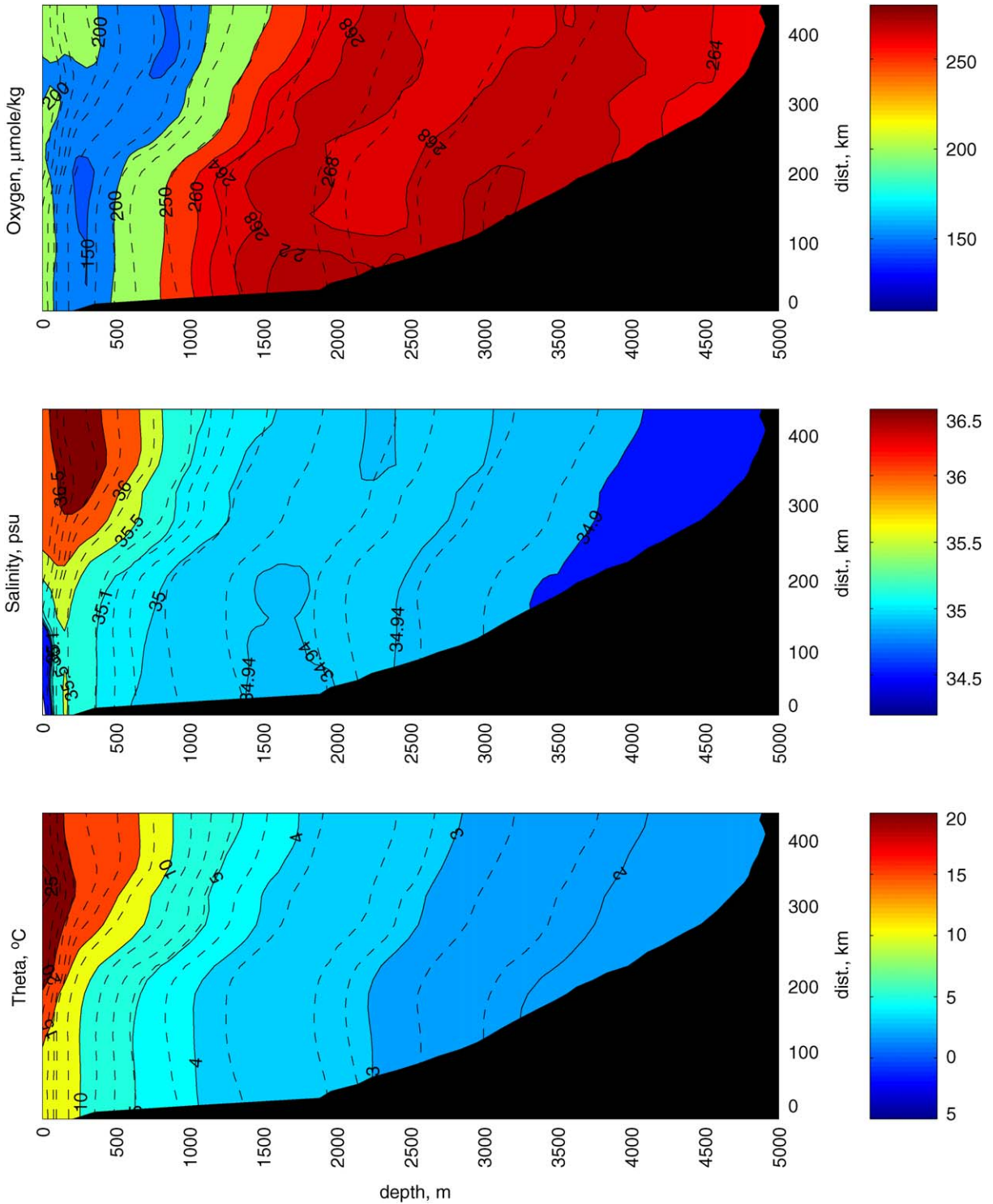


Fig. 2. Mean property sections from the CTD data shown relative to a shelf break origin and along a line defined by the aggregate of the stations (Fig. 1). Potential Temperature (left), Salinity (center) and Dissolved Oxygen (right). Solid lines and colors represent each of the different variables plotted, while dashed lines are neutral density surfaces (see Fig. 3, center).

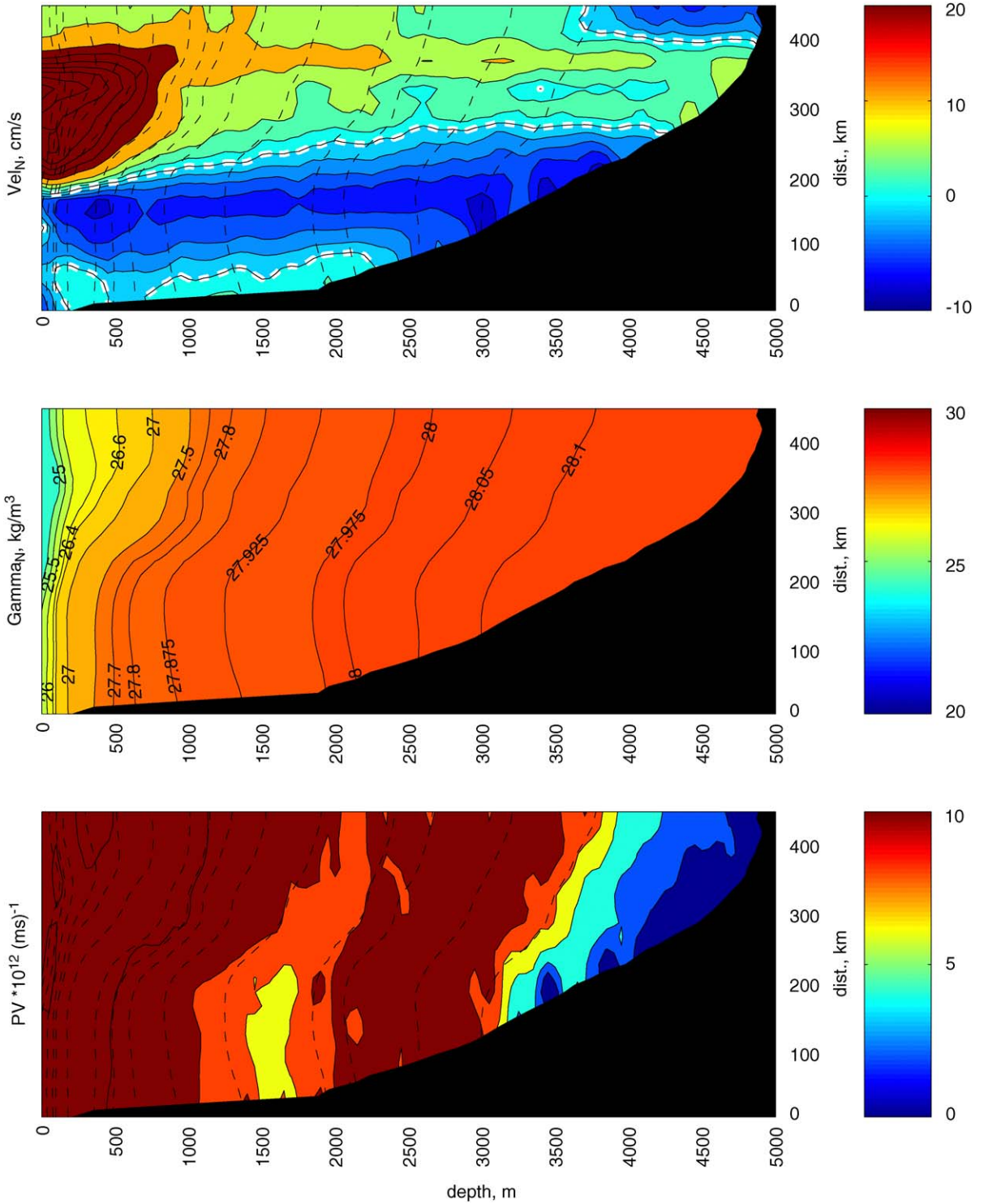


Fig. 3. Planetary Potential Vorticity (left) is plotted on a scale that illustrates the low PV values in LSW and the sharp gradient of PV found between the Overflow Waters and the underlying LDW. Neutral Density (center) and Normal Velocity (right) are also given. For the latter, the thick dashed contour is for zero velocity and positive values are poleward.

of 5 cm/s, can cause substantial variability in the observed velocity in this region. Since several of our sections have a limited number of stations (Table 1), spatial filtering was not done prior to ensemble averaging individual current profiles. We have relied on enough members of the ensemble to remove the TRW influence. However, as the distribution of stations is not homogeneous, the TRW elimination is better closer to shore, where there are more stations. Estimates of the mapping error (not shown) indicate errors of 0.8 cm/s below the surface layer and inshore of the 2000 m isobath, with slightly lower values within the equatorward flow between this isobath and the Gulf Stream, and larger errors within the surface and deep Gulf Stream. Since the TRW-induced noise is low mode, vertical averaging will not eliminate its influence, whereas lateral averaging will. For our section-averaged transports, we estimate this transport ‘error’ to be of order 2 Sv ( $1 \text{ Sv} = 10^6 \text{ m}^3/\text{s}$ ) for the layer of NADW. We will later see that other factors can induce comparable uncertainty in layer transports.

On the inshore side of the Gulf Stream, the mean flow is in the opposite direction. Velocities there are much weaker than the Gulf Stream near the surface and more barotropic, with little *vertical* variation that can be linked with *vertical* changes in water masses through the deep layers flowing towards the equator, except perhaps for a slight increase in equatorward flow within the Overflow waters at 3500 m depth. The equatorward flowing waters of LSW origin are clearly more “pristine” than the poleward flowing counterparts, having more intense tracer signatures, although one might argue that some LSW is actually moving to the north within the deep Gulf Stream. We will say more about this later, as it is linked to deep recirculation. Most of the equatorward flow is found between the 2500 and 4000 m isobaths. In the deepest levels at the offshore end of the section, there is a suggestion of increased equatorward flow again, but we hasten to point out that beyond the 4500 m isobath, our ensemble amounts to only one occupation of the section! On the inshore side of the section inside of the 2500 m isobath, flows are weak, and for a small segment of the section, again positive, but with weak mean flows (1 cm/s) that

are not significantly different from zero, and little volume transport, as we shall soon see.

### 3. Transports

We have defined three layers by their neutral density (Table 2), and will focus mainly on the flow of the deeper two layers: one containing various types of LSW, and one containing Overflow Water as well as LDW, which is a mixture of Overflow and Antarctic Bottom Water. Volume transports for 20-km-wide distance cells are estimated for each of these layers (Fig. 4) as well as their cumulative transport starting at the shelf break origin. Near the upper slope, currents are northerly but weak, with small, insignificant net transports of less than 0.2 Sv. Beginning at about the 2500 m isobath, at a distance of ca. 100 km, LSW transport is equatorward, reaching its maximum cumulative transport of 7.5 Sv at a distance/depth of 200 km/3700 m. The Overflow/LDW layer has a maximum transport in deeper water: it reaches its maximum cumulative equatorward transport of 12.5 Sv at a distance/depth of ca. 260 km/4200 m. Because of the different phasing of the two layers, the sum of the two reaches its maximum cumulative transport of  $-19 \text{ Sv}$ , midway between the above two locations.

The deep flow of the Gulf Stream, which we have only sampled on two cruises, eventually overcomes the equatorward transport in the DWBC. The outer boundary of our section is not the point beyond which there is no deep flow. So it would be incorrect to assume that the accumulated transports shown are net transports across a section between Cape Cod and Bermuda. Our focus with the present data set is with the deep equatorward flow along the

Table 2  
Neutral density layers used to define volume transport

Layer#	Neutral Density Range ( $\text{kg}/\text{m}^3$ )	Comment
1	25.000: 27.800	Upper water
2	27.800: 27.975	Upper and classical LSW
3	27.975: 28.140	Overflow, LDW

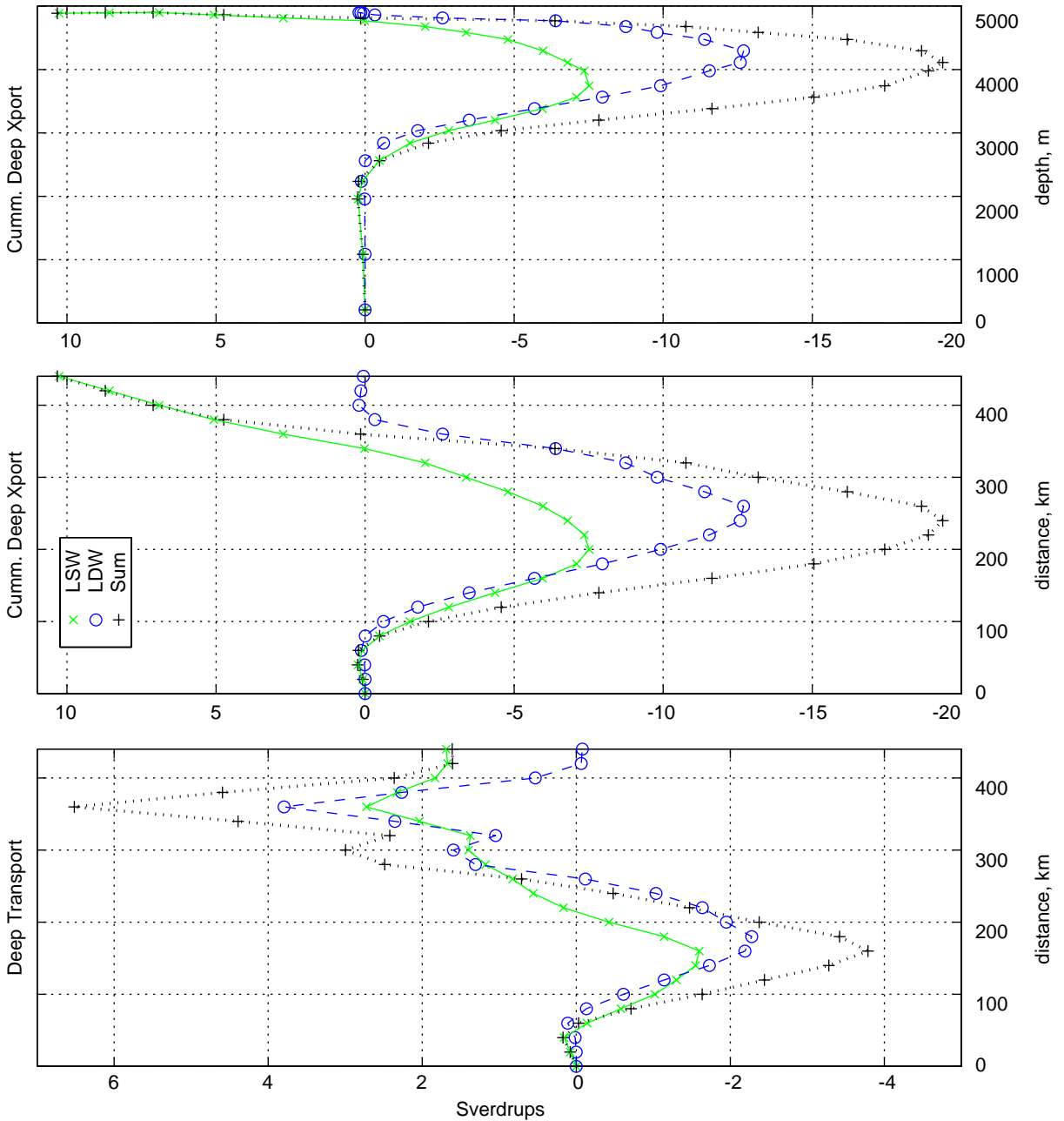


Fig. 4. Layer-averaged transport (left panel) and cumulative transport (right panels) in neutral density layers encompassing LSW (solid lines and x's), Overflow and LDW (dashed lines and circles), and their sum (dotted lines and pluses). Cumulative transport (in Sv, = 10<sup>6</sup> m<sup>3</sup>/s) is initialized at the shelf break and plotted against offshore distance (left two panels) and water depth (right panel).

steep bathymetry of the continental slope. The DWBC we find there is well-defined by the present data set, but we can say little here about offshore

recirculation, except to note that it occurs, as can be readily seen with the poleward transport of diluted LSW and Overflow/LDW in the Gulf Stream.

We also have calculated the transport of the upper layer and for the whole water column, a cumulative transport of  $-18\text{ Sv}$  at 200 km and  $+84\text{ Sv}$  at the offshore edge. The net transport of the Gulf Stream would be the difference of these two numbers ( $102\text{ Sv}$ ) if our outer boundary were across all of the Gulf Stream. While our total transport figure is intermediate between those at 73 W ( $93.7\text{ Sv}$ ) and 68 W ( $112.8\text{ Sv}$ ) according to [Johns et al. \(1995\)](#), it is most probably underestimated.

#### 4. Effect of warm-core rings on DWBC

Our ensemble mean property section excludes data from one of the available cruises: EN311. During this cruise, a Warm-Core Ring (WCR) is located along the station line ([Fig. 5](#)). Substantial flow anomalies are present throughout the water column. Upper ocean flows are anticyclonic and generally follow what one would infer from the sea-surface temperature imagery (e.g., [Joyce, 1984](#)). Deep flows are in the opposite direction from the long-term ensemble mean previously shown. It is clear from this one example that WCRs are capable of disrupting the flow in the DWBC. In another example ([Amy Bower, personal comm., 2004](#)), deep (3000 m) floats have been observed to be displaced within the DWBC by a WCR and in some cases completely leave the deep flow along the continental slope. Our EN311 section did not go offshore far enough to determine if the DWBC flow was completely blocked or merely diverted around the southern periphery of the ring. In the latter case, the WCR would not alter DWBC transports, only where they are found. With these problematic EN311 stations, amounting to about 10% of our total stations, one might be able to better gauge the overall effect of WCRs on DWBC transport if we also knew how often a WCR was over the section and how typical were our EN311 flow observations. On the former point, we can make use of the [Brown et al. \(1986\)](#) estimates of WCR probability density structure for a swath 50 km wide (roughly one ring radius) along the line of our section of length 200 km in the Slope Water. We estimate a

probability of 0.2 that on any given day a WCR will be found within this area. This is quite high, higher than the percentage of stations made when a WCR was present, and suggests that the following lower DWBC transport estimate may be closer to the truth than our upper. However, without a better knowledge of the circulation anomalies caused by WCRs, we have little confidence that our single realization can be regarded as 'typical'. If EN311 is merely included as if it were like all of the other cruises, one can see its effect on transport to gauge what might be the range of uncertainty of DWBC transport ([Fig. 6](#)). The range in the total deep transport (black lines) amounts to  $-19\text{ Sv}$  (w/o the WCR) to  $-14\text{ Sv}$  with the WCR. For simplicity, we estimate the transport of the DWBC to be  $-16.5 \pm 2.5\text{ Sv}$ , with the 'error' associated with effects due to WCRs. This uncertainty is comparable to what we estimate could arise due to other variability, such as TRWs.

#### 5. Discussion

The transport numbers for our section are close to those of [Pickart and Smethie \(1998\)](#), who estimated a DWBC transport of  $-18.9\text{ Sv}$  at  $55^\circ\text{W}$ . Yet our transport structure is only weakly tied vertically and horizontally to structure of the water masses. Thus our result is intermediate to [Pickart and Smethie \(1998\)](#) and [Leaman and Harris \(1990\)](#). In the latter, tracer and velocity cores are not coincident. All three locations must address the issue of recirculation. Our section is at the extreme western edge of the northern recirculation gyre, and according to [Hogg et al. \(1986\)](#), this gyre is found in deeper water between the Gulf Stream and the continental slope. Yet clearly there is some recirculation occurring within and to the southeast of the Gulf Stream at our  $70^\circ\text{W}$  section. Deep LSW and Overflow waters can be seen heading back towards their northern sources within the deep Gulf Stream. Deep recirculation on the seaward side of the Gulf Stream is also a feature of the western N. Atlantic ([Worthington, 1976](#)). The pathway by which the DWBC crosses under the Gulf Stream (e.g., [Pickart and Smethie, 1993](#)) involves not only these deep recirculation

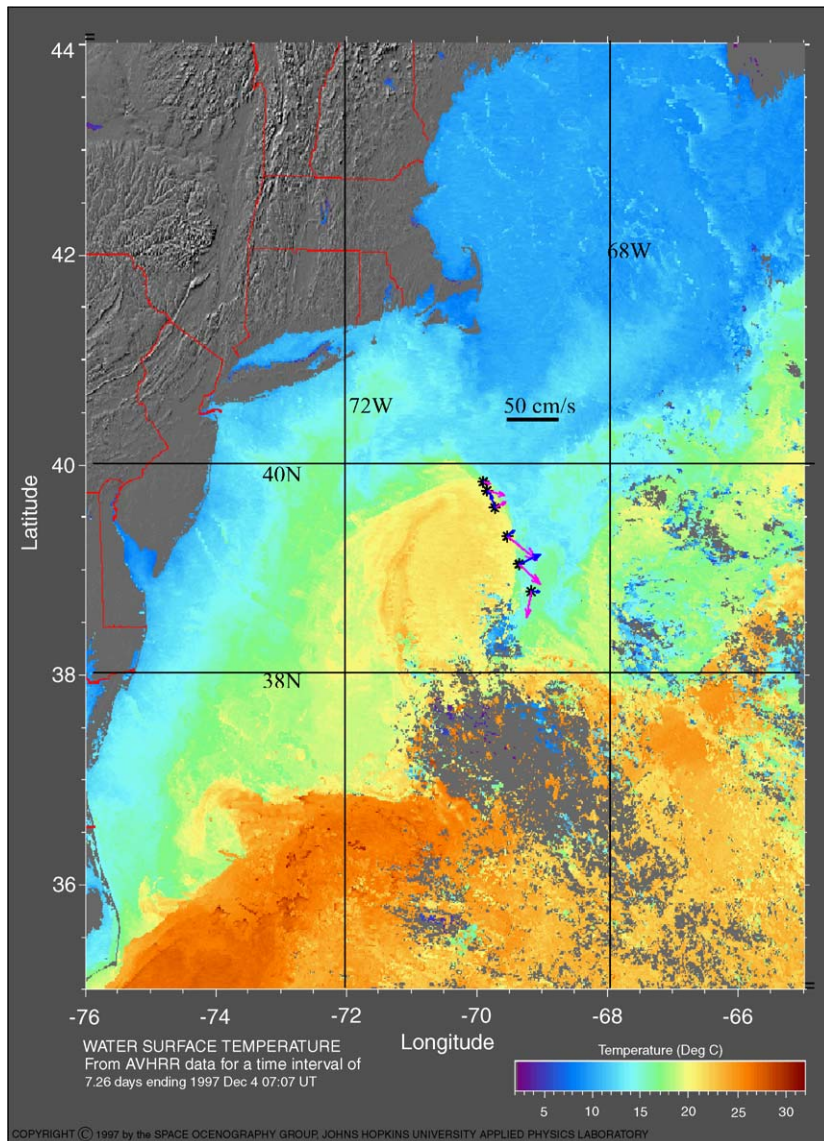


Fig. 5. SST image (from the Johns Hopkins University, Applied Physics Laboratory website) showing a composite SST image for 1–7 December 1997 and hydrographic stations taken during EN311 from 2–4 December. Magenta vectors are from LADCP data averaged in the upper 200 m and blue vectors are averages between 1500 m depth and the local bottom.

gyres, but also time dependence, allowing tracers to cross ‘mean’ streamlines.

The equatorward-flowing waters are confined between water depths of 2500 and 4000 m, and while there is some slight tilt to the isolines in the plane of the section and a slight increase in equatorward flow of the Overflow water, the flow

in the DWBC at 70°W is barotropic in nature, and thus largely invisible to normal hydrography. This illustrates the value of the direct velocity observations in defining the structure and amplitude of this flow. Inshore of the 2500 m isobath, flow rates in the LSW layer decrease, while the tracer signature does not, in contrast to the observations

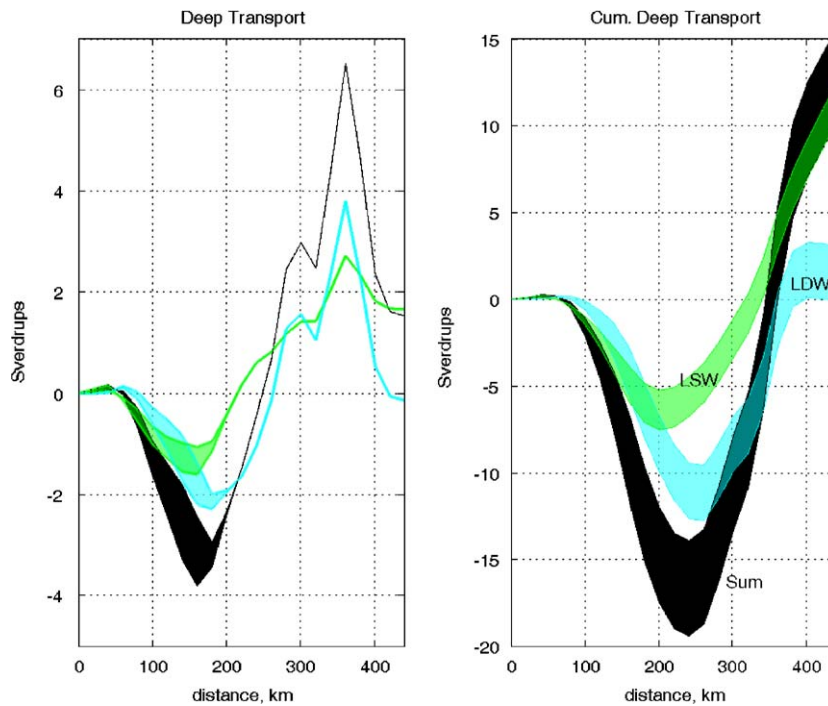


Fig. 6. Deep Layer-averaged transports (as in Fig. 4) with and without the EN311 section, which includes a WCR. Generally, the presence of the WCR reduced deep southward transports and this defines the low transport branch in the two panels, which show transport in 20-km-wide portions of the section (left) and accumulated transport (right). The shaded regions therefore represent uncertainty in transport due to rings.

further upstream at 55°W, where LSW characteristics and flow are greatest on the boundary. Inshore of the 4000 m isobath, the total, vertically averaged equatorward transport is 25 Sv.

Our equatorward transport of NADW in the DWBC amounts to  $16.5 \pm 2.5$  Sv. To what extent does this represent the total cold water transport in the thermohaline circulation? Schmitz and McCartney (1993) estimate that a total of about 16 Sv of LSW and Overflow/LDW are exported to the south from the subpolar gyre. While this would seem to fit well with our estimate, we note that 4 Sv of their flow is so deep that it cannot pass between Bermuda and the continental slope, and so must go around the eastern edge of the Bermuda Rise and rejoin the DWBC between our location and Abaco. Schott et al. (2004) estimate at 50°W from hydrographic, LADCP, and moored current meter records, that approximately 13 Sv of NADW is exported from the subpolar gyre in the DWBC.

(We use their upper potential density limit of  $\sigma_\theta = 27.68 \text{ kg/m}^3$ , which is equivalent to our upper bound of  $\gamma_n = 27.8 \text{ kg/m}^3$  using neutral density.) Their transport figure is lower than the Schmitz & McCartney estimate and less than that published by Pickart and Smethie at 55°W. The situation at Abaco contrasts the large DWBC transport of Leaman and Harris (1990) with that of Lumpkin and Speer (2003), who estimate that  $17.6 \pm 2.7$  Sv of NADW is transported equatorward across 24°N. In the latter, slightly different neutral density levels were used to identify NADW, and the best-constrained transport figure is for the section mean, not the DWBC itself. Because of the hydrographic sections used in their inverse model, they can provide no estimate closer to the latitude of our section for further comparison. Thus, it would appear that there is no previously published DWBC transport figure for our 70°W section south of Cape Cod, but given the error bars in

various estimates, our results at 70°W are generally consistent with what is known for the western N. Atlantic.

### Acknowledgements

We wish to acknowledge the support of NSF Grant OCE-0241354, and velocity data provided from site “W” (J. Toole) and from the KN173 leg 2 (Martin Visbeck). This is WHOI contribution #11162.

### References

- Brown, O.B., Cornillon, P.C., Emmerson, S.R., Carle, H.M., 1986. Gulf Stream warm rings: a statistical study of their behavior. *Deep-Sea Research* 33, 1459–1474.
- Doherty, K.W., Frye, D.E., Liberatore, S.P., Toole, J.M., 1999. A moored profiling instrument. *Journal of Atmospheric and Oceanic Technology* 16, 1816–1829.
- Fine, R., Molinari, R.L., 1988. A continuous deep western boundary current between Abaco (26.5°N) and Barbados (13°N). *Deep-Sea Research* 35, 1441–1450.
- Fischer, J., Visbeck, M., 1993. Deep profiling with self-contained ADCPs. *Journal of Atmospheric and Oceanic Technology* 10, 764–773.
- Hogg, N.G., Pickart, R.S., Hendry, R.M., Smethie Jr, W.J., 1986. The Northern Recirculation Gyre of the Gulf Stream. *Deep-Sea Research* 33, 1139–1165.
- Johns, W.E., Shay, T.J., Bane, J.M., Watts, D.R., 1995. Gulf Stream structure, transport, and recirculation near 68°W. *Journal of Physical Oceanography* 100, 817–838.
- Joyce, T.M., 1984. Velocity and hydrographic structure of a Gulf stream warm-core ring. *Journal of Physical Oceanography* 14, 936–947.
- Leaman, K.D., Harris, J.E., 1990. On the average absolute transport of the deep western boundary currents east of Abaco Island, the Bahamas. *Journal of Physical Oceanography* 20, 467–475.
- Lumpkin, R., Speer, K., 2003. Large-scale vertical and horizontal circulation in the North Atlantic Ocean. *Journal of Physical Oceanography* 33, 1902–1920.
- Pickart, R.S., Smethie Jr., W.M., 1993. How does the deep western boundary current cross the Gulf Stream? *Journal of Physical Oceanography* 23, 2602–2616.
- Pickart, R.S., Smethie Jr, W.M., 1998. Temporal evolution of the deep western boundary current where it enters the subtropical domain. *Deep-Sea Research I* 45, 1053–1083.
- Schmitz Jr., W.J., McCartney, M.S., 1993. On the North Atlantic Circulation. *Reviews of Geophysics* 31, 29–49.
- Schott, F.R., Zantopp, R., Stramma, L., Dengler, M., Fischer, J., Wibaux, M., 2004. Circulation and Deep-Water export at the Western exit of the subpolar North Atlantic. *Journal of Physical Oceanography* 34, 817–843.
- Worthington, L.V., 1976. On the North Atlantic Circulation. *The Johns Hopkins Oceanographical Studies* 6, 110.